Chapter 1

Scattering of Nucleons

"Although the study of the deuteron gives us a number of clues about the nucleon–nucleon interaction, the total amount of information available is limited... To study the nucleon–nucleon interaction in different configurations, we can perform nucleon–nucleon scattering experiments."

K. S. Krane

The deuteron (Lectures 7–9) is the only bound two-nucleon system. It samples the residual NN force in a single channel, mostly ${}^3S_1$ with a few-percent D-wave, at a fixed average separation fixed by weak binding. That is not enough to reconstruct the full force. There are no bound excited states to explore other partial waves or spin orientations, and the continuum is invisible from multipole moments alone [6].

Scattering supplies what the bound state cannot: controllable energy, access to $\ell = 0, 1, 2, \ldots$, and both spin channels. In this lecture the experimental definition of the cross section is tied to partial-wave analysis. Phase shifts δ_ℓ become the language in which theory and experiment meet for a short-range central potential [6, 1, 2, 14].

1.1 Why scatter neutrons on protons?

A scattering experiment uses a monoenergetic **projectile** beam and a **target** with many scattering centres. For n–p scattering the projectiles are neutrons of chosen kinetic energy and the target is hydrogen: each scattering centre is a free proton (bound only in the atom, irrelevant at nuclear energies). A detector at polar angle θ relative to the beam axis counts scattered particles. For a central force the yield does not depend on the azimuthal angle ϕ.

Hydrogen is essential for a clean NN measurement. On a heavy nucleus an incident nucleon would scatter from several target nucleons within the force range, so the observed yield would mix many-body effects. On hydrogen each encounter is a single np collision; multiple scattering from different atoms is rare if the target is thin [6]. The same philosophy motivates electron scattering on thin foils when one wants the elementary charge form factor (Lecture 1): isolate one interaction per projectile.

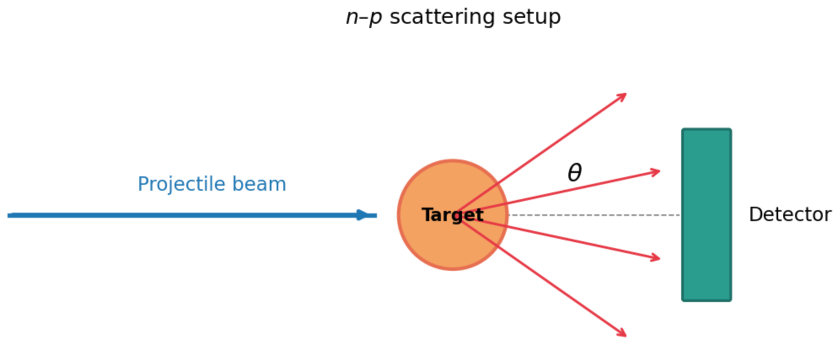

Figure 1.1: Schematic n–p scattering setup: monoenergetic projectile beam, hydrogen target, and detector at angle θ.

1.2 Differential and total cross sections

The number $\mathrm{d}N$ of particles recorded in time t into solid angle $\mathrm{d}\Omega$ grows with exposure time, detector acceptance, beam intensity I (particles per unit area per unit time), and the number of target centres N_t (or areal density n_a times the illuminated area). These experimental knobs are factored out by defining the **differential scattering cross section** $\mathrm{d}\sigma/\mathrm{d}\Omega$ through

$$\mathrm{d}N = \frac{\mathrm{d}\sigma}{\mathrm{d}\Omega}\, t\, \mathrm{d}\Omega\, I\, N_t. \tag{1.1}$$

Equivalently,

$$\frac{\mathrm{d}\sigma}{\mathrm{d}\Omega} = \frac{\mathrm{d}N}{\mathrm{d}\Omega\, n_a\, N_p}, \qquad N_p = tIA, \tag{1.2}$$

with A the beam area. The cross section has dimensions of area; the historical unit is the barn,

$$1\,\mathrm{b} = 10^{-28}\,\mathrm{m}^2 = 100\,\mathrm{fm}^2.$$

Nuclear NN cross sections at low energy are tens of barns, huge compared with the geometric size of a nucleon ($\sim 1\,\mathrm{fm}^2$), a quantum enhancement characteristic of low-energy s-wave scattering [6, 1].

Physically, $\mathrm{d}\sigma/\mathrm{d}\Omega$ is the effective area that the target presents for scattering into $\mathrm{d}\Omega$. It packages all of the unknown dynamics into a measurable quantity: once $\mathrm{d}\sigma/\mathrm{d}\Omega$ is known, one can compare theories without redoing the experiment for every proposed potential.

Angles and energies may be quoted in the laboratory or centre-of-mass (CM) frame. Partial-wave formulae below are written in the CM frame; converting to laboratory angles for equal-mass np scattering is a standard kinematic exercise. The **total** elastic cross section is the angular integral

$$\sigma_{\text{tot}} = \int \frac{\mathrm{d}\sigma}{\mathrm{d}\Omega}\, \mathrm{d}\Omega. \tag{1.3}$$

For pure s-wave scattering, $\mathrm{d}\sigma/\mathrm{d}\Omega$ is isotropic in the CM frame and $\sigma_{\text{tot}} = 4\pi\,(\mathrm{d}\sigma/\mathrm{d}\Omega)$.

1.3 Central potential, plane waves, and partial waves

A **central** potential $V(r)$ depends only on the nucleon–nucleon separation. Angular momentum about the force centre is then conserved, so eigenstates of definite orbital angular momentum ℓ are useful. In the absence of interaction the incident beam is a plane wave along z,

$$\psi_{\text{inc}} = e^{ikz}, \qquad k = \frac{p}{\hbar} = \frac{\sqrt{2\mu E}}{\hbar}, \tag{1.4}$$

where $\mu \approx m_N/2$ is the reduced mass of the NN system and E is the centre-of-mass kinetic energy. Multiplying by $e^{-iEt/\hbar}$ makes the wave travel in the $+z$ direction: toward the target for $z < 0$ and away from it for $z > 0$ [6].

A plane wave has definite energy and momentum along z, but it is *not* an eigenstate of $\boldsymbol{L}^2$. It is a coherent superposition of all orbital angular momenta. Because of axial symmetry about the beam, only projections $m = 0$ appear. The expansion in spherical waves (partial waves) reads

$$e^{ikz} = \sum_{\ell=0}^{\infty} i^{\ell}(2\ell+1)\, j_\ell(kr)\, P_\ell(\cos\theta), \tag{1.5}$$

where j_ℓ are spherical Bessel functions and P_ℓ Legendre polynomials. Each term $\ell = 0, 1, 2, \dots$ is an s, p, d, … wave with a definite impact-parameter character in the semiclassical picture.

1.4 Phase shifts: what a short-range potential can do

Detectors sit centimetres from the target, while the nuclear force acts only for $r \lesssim$ a few fm. Outside the force range the wave is free again; the potential cannot change its wavelength there. What it *can* do is shift the phase of each outgoing partial wave relative to the free solution.

Free spherical waves have the asymptotic form

$$j_\ell(kr) \sim \frac{\sin(kr - \ell\pi/2)}{kr} \qquad (kr \to \infty). \tag{1.6}$$

In the presence of a short-range central potential the radial function $u_\ell(r) = rR_\ell(r)$ for r larger than the force range becomes

$$u_\ell(r) \sim \sin(kr - \ell\pi/2 + \delta_\ell), \tag{1.7}$$

where $\delta_\ell(E)$ is the **phase shift** in channel ℓ [6, 2]. Attractive potentials typically pull nodes of u_ℓ toward the origin (positive δ_ℓ); repulsive potentials push nodes outward (negative δ_ℓ).

All information about $V(r)$ that elastic scattering at energy E can provide is encoded in the set $\{\delta_\ell(E)\}$. Solving the radial Schrödinger equation for a model potential and reading δ_ℓ is the theoretical route; measuring $\mathrm{d}\sigma/\mathrm{d}\Omega$ and fitting δ_ℓ is the experimental route. Phase shifts themselves are not directly observed: they are a convenient parameterisation of the measured cross sections (and polarisations). The two routes meet in (1.11) below.

For $\ell = 0$ one may write the exterior wave as a combination of incoming and outgoing spherical waves $e^{\pm ikr}/r$. Scattering does not create or destroy particles in elastic scattering, so it cannot change the *amplitudes* of those waves; it can only change the relative phase of the

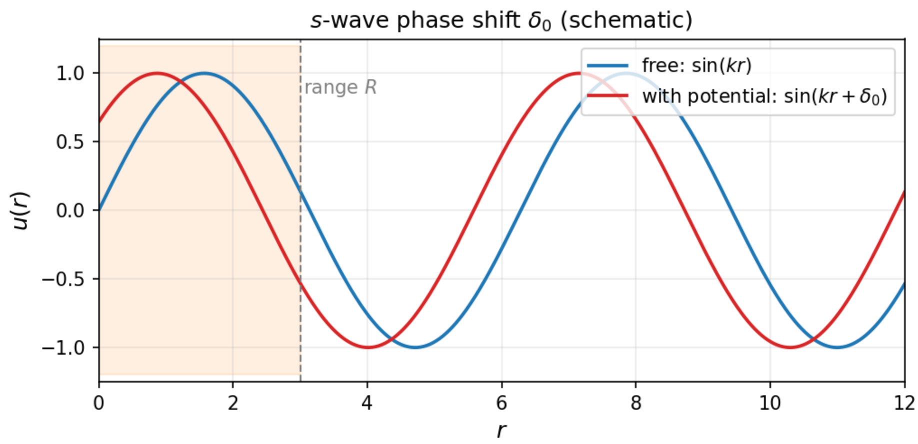

Figure 1.2: Schematic s-wave radial wave $u(r)$. Inside the force range the potential distorts the wave; outside, the free oscillation is shifted by the phase δ_0.

outgoing piece. That single phase is δ_0 (up to a conventional factor of two in intermediate steps of the algebra) [6].

1.5 Cross section from phase shifts

Matching the asymptotic partial-wave solution to an incident plane wave plus outgoing scattered spherical wave produces the scattering amplitude $f(\theta)$. Outside the force range the radial wave in channel ℓ may be written as a superposition of incoming and outgoing spherical waves,

$$u_\ell(r) \propto e^{-i(kr-\ell\pi/2)} - S_\ell\, e^{i(kr-\ell\pi/2)}, \tag{1.8}$$

with the unitary S-matrix element $S_\ell = e^{2i\delta_\ell}$ for a real central potential (elastic scattering). The coefficient of the outgoing scattered wave relative to the free case defines the partial-wave amplitude

$$f_\ell = \frac{S_\ell - 1}{2ik} = \frac{e^{2i\delta_\ell} - 1}{2ik} = \frac{e^{i\delta_\ell}\sin\delta_\ell}{k}. \tag{1.9}$$

Summing over partial waves with the Legendre weights of the plane-wave expansion gives

$$f(\theta) = \sum_{\ell=0}^{\infty}(2\ell+1)\, f_\ell\, P_\ell(\cos\theta) = \frac{1}{k}\sum_{\ell=0}^{\infty}(2\ell+1)\, e^{i\delta_\ell}\sin\delta_\ell\, P_\ell(\cos\theta). \tag{1.10}$$

The CM differential cross section is therefore

$$\frac{\mathrm{d}\sigma}{\mathrm{d}\Omega} = |f(\theta)|^2 = \frac{1}{k^2}\left|\sum_{\ell=0}^{\infty}(2\ell+1)\, e^{i\delta_\ell}\sin\delta_\ell\, P_\ell(\cos\theta)\right|^2. \tag{1.11}$$

(The overall phase convention for $e^{i\delta_\ell}$ varies among sources; the measurable $|f|^2$ is fixed by the δ_ℓ.) The factor $(2\ell+1)$ counts magnetic substates of a given ℓ; the Legendre polynomials build the angular pattern of each partial wave.

When only $\ell = 0$ contributes, $P_0 = 1$ and

$$\frac{\mathrm{d}\sigma}{\mathrm{d}\Omega} = \frac{\sin^2 \delta_0}{k^2}, \tag{1.12}$$

independent of angle in the CM frame. Integrating over 4π and using the orthogonality $\int P_\ell P_{\ell'} \, \mathrm{d}\Omega = 4\pi\delta_{\ell\ell'}/(2\ell+1)$ gives the total cross section

$$\sigma_{\text{tot}} = \frac{4\pi}{k^2} \sum_{\ell=0}^{\infty} (2\ell+1) \sin^2 \delta_\ell = \frac{4\pi}{k^2} \sin^2 \delta_0 \quad (s\text{-wave only}). \tag{1.13}$$

Thus a single number $\delta_0(E)$ determines the entire low-energy elastic yield. The unitarity bound $\sin^2 \delta_0 \leq 1$ implies $\sigma_{\text{tot}} \leq 4\pi/k^2$: at very low energy the quantum cross section can greatly exceed the geometric size of the potential well [6, 14].

For equal-mass np scattering the laboratory and CM scattering angles are related by $\theta_{\text{lab}} = \theta_{\text{CM}}/2$, and

$$\left(\frac{\mathrm{d}\sigma}{\mathrm{d}\Omega}\right)_{\text{lab}} = 4 \cos\theta_{\text{lab}} \left(\frac{\mathrm{d}\sigma}{\mathrm{d}\Omega}\right)_{\text{CM}}. \tag{1.14}$$

Partial-wave formulae in this lecture are always in the CM frame unless stated otherwise.

Key idea

Phase shifts δ_ℓ are the interface between potential and data. Theory: solve the radial equation for $V(r)$ and extract δ_ℓ. Experiment: measure $\mathrm{d}\sigma/\mathrm{d}\Omega$ and determine δ_ℓ.

1.6 Low energy: only s-wave scattering

Semiclassically, a projectile of momentum $p = \sqrt{2\mu E}$ that grazes the force range r_0 carries angular momentum $\ell\hbar \sim pr_0$. For nuclear $r_0 \sim 2\,\text{fm}$ and $E \sim 1\,\text{MeV}$ one finds $pr_0/\hbar \ll 1$: the projectile cannot bring $\ell \geq 1$ inside the nuclear force range without flying past outside the well. Only $\ell = 0$ scatters. At $E \sim 10\,\text{MeV}$, $\ell = 1$ begins to contribute [6].

A sharper estimate uses the free kinetic energy scale associated with confinement in a well of size R,

$$T \sim \frac{\ell(\ell+1)\hbar^2}{2\mu R^2}.$$

For $\ell = 1$, $R \sim 1\,\text{fm}$, and $\mu c^2 \sim 500\,\text{MeV}$, T is tens of MeV. Incident energies far below that scale justify the s-wave truncation [6].

This is why low-energy np data are so powerful and so simple: a single phase $\delta_0(E)$ (actually one for each spin channel) carries the dynamics, and $\sigma(\theta)$ is nearly isotropic.

1.7 Square well in the continuum: matching for $E > 0$

The same square well used for the deuteron bound state can be solved for positive energy. For $\ell = 0$,

$$V(r) = \begin{cases} -V_0 & r < R, \\ 0 & r > R, \end{cases} \qquad E > 0. \tag{1.15}$$

Inside, $u(r) = A\sin(k_1 r)$ with $k_1 = \sqrt{2\mu(V_0 + E)}/\hbar$ (regularity at the origin again kills the cosine). Outside,

$$u(r) = C\sin(kr + \delta_0), \qquad k = \frac{\sqrt{2\mu E}}{\hbar}. \tag{1.16}$$

Continuity of u and u' at $r = R$ yields

$$k\cot(kR + \delta_0) = k_1\cot(k_1 R). \tag{1.17}$$

Solving for the phase shift,

$$\delta_0 = \arctan\!\left(\frac{k}{k_1}\tan(k_1 R)\right) - kR \pmod{\pi}. \tag{1.18}$$

Given E, V_0, and R, one thus obtains $\delta_0(E)$ and then predicts σ_{tot} from (1.13) [6].

In the zero-energy limit $k \to 0$, $k_1 \to K \equiv \sqrt{2\mu V_0}/\hbar$ and the scattering length extracted from $a = -\lim(\tan\delta_0/k)$ becomes

$$a = R - \frac{\tan(KR)}{K}. \tag{1.19}$$

(If $KR = \pi/2$, $a \to \infty$: the zero-energy bound-state threshold of Lecture 7.) Then $\sigma_{\text{tot}} \to 4\pi a^2$.

As $V_0 \to 0$, $\delta_0 \to 0$ and there is no scattering. For the attractive well fitted to the deuteron ($V_0 \approx 35\,\text{MeV}$, $R \sim 2\,\text{fm}$), low-energy δ_0 is large and σ_{tot} is tens of barns. Experiment finds the zero-energy unpolarised *np* cross section near 20 b, not the $\sim$ 4–5 b that a pure triplet estimate would suggest. The resolution is that free protons and neutrons scatter in a statistical mixture of triplet and singlet spins: three triplet states and one singlet, so the spin weights are 3/4 and 1/4. Writing

$$\sigma = \tfrac{3}{4}\sigma_t + \tfrac{1}{4}\sigma_s, \tag{1.20}$$

and taking $\sigma_t \approx 4\pi a_t^2 \sim 4.6\,\text{b}$ from the deuteron (triplet) channel leaves $\sigma_s \sim 70\,\text{b}$: the singlet interaction is strong but just unbound, producing a large negative scattering length [6, 14].

1.8 Scattering length and effective range

At vanishing energy, $\delta_0 \to 0$ in such a way that

$$a = -\lim_{k\to 0}\frac{\tan\delta_0}{k} \tag{1.21}$$

defines the **scattering length** a. From $\sigma_{\text{tot}} = (4\pi/k^2)\sin^2\delta_0$ and $\sin\delta_0 \approx \tan\delta_0 \approx -ka$ one obtains

$$\sigma_{\text{tot}} \to 4\pi a^2. \tag{1.22}$$

The sign of a carries physics: a large *positive* scattering length is characteristic of a barely bound state (triplet, deuteron); a large *negative* scattering length signals a virtual state just above threshold (singlet) [6, 14].

Checked low-energy np numbers

Standard values are $a_t \approx +5.4\,\text{fm}$ (triplet) and $a_s \approx -23.7\,\text{fm}$ (singlet). The unpolarised zero-energy cross section is then

$$\begin{aligned}\sigma &= 4\pi\left(\tfrac{3}{4}a_t^2 + \tfrac{1}{4}a_s^2\right)\\ &= 4\pi\left(\tfrac{3}{4}(5.4)^2 + \tfrac{1}{4}(23.7)^2\right) \approx 4\pi(21.9 + 140.4) \approx 20\,\text{b},\end{aligned}$$

matching experiment. The huge singlet piece dominates because $|a_s|$ is so large: the singlet potential nearly binds [6, 14].

A more accurate low-energy expansion follows from matching the exterior wave to an effective-range expansion of the logarithmic derivative. Writing

$$k\cot\delta_0 = -\frac{1}{a} + \frac{1}{2}r_0k^2 + \cdots, \tag{1.23}$$

defines the effective range r_0 of fermi size. The first two terms already reproduce low-energy $\delta_0(E)$ in each spin channel without committing to a full potential at every energy [6, 14]. Fitting a and r_0 is how modern analyses encode low-energy NN physics.

Key idea

The deuteron fixes the *triplet* well near threshold. Scattering reveals a strong *singlet* interaction that fails to bind, and it maps how $\delta_\ell(E)$ evolve as higher partial waves open with energy.

1.9 Further physics: coherent scattering and spin channels

At very low energy the de Broglie wavelength of a neutron can exceed the size of a hydrogen molecule. Scattering from the two protons then interferes coherently, and the cross sections of ortho- and parahydrogen differ because the total proton spin of the molecule weights triplet and singlet np amplitudes differently. That difference is direct evidence that $\sigma_t \neq \sigma_s$ [6].

The optical analogy remains useful: an attractive well of nuclear size diffracts the incident wave much as an obstacle of size R diffracts light of wavelength $\lambda \sim 2\pi/k$. Partial-wave analysis is the quantum bookkeeping of that diffraction pattern, partial wave by partial wave.

1.10 Problems with solutions

Problem 10.1 — Cross section dimensions

From $\mathrm{d}N = \sigma\, t\, \mathrm{d}\Omega\, I\, N_t$, show that σ has dimensions of area.

Solution 10.1

$\mathrm{d}N$ is dimensionless (a count). tI has dimensions of (time)×(area^{-1} time^{-1})=area^{-1}; N_t is a number; $\mathrm{d}\Omega$ is dimensionless. Hence σ must supply an area so that the product is dimensionless.

Problem 10.2 — Low-energy total cross section

At low energy only δ_0 is nonzero. Show that $\sigma_{\text{tot}} = 4\pi k^{-2}\sin^2\delta_0$. If $\delta_0 = \pi/2$, what is σ_{tot}?

Solution 10.2

Integrate the isotropic $\sigma(\theta) = \sin^2\delta_0/k^2$ over 4π:

$$\sigma_{\text{tot}} = \frac{4\pi}{k^2}\sin^2\delta_0.$$

At resonance-like $\delta_0 = \pi/2$, $\sigma_{\text{tot}} = 4\pi/k^2$ (unitarity limit for s-wave) [6].

Problem 10.3 — Why only s-wave at $1\,\text{MeV}$

Estimate $\ell_{\max} \sim pr_0/\hbar$ for $E = 1\,\text{MeV}$ (lab-scale NN), $r_0 = 2\,\text{fm}$, $\hbar c = 200\,\text{MeV fm}$, $\mu c^2 \approx 500\,\text{MeV}$. Argue that $\ell = 0$ dominates.

Solution 10.3

$$pc = \sqrt{2\mu c^2\, E} \approx \sqrt{1000\,\text{MeV}^2} \approx 32\,\text{MeV}, \qquad \frac{pr_0}{\hbar} = \frac{(pc)\, r_0}{\hbar c} \approx \frac{32\times 2}{200} \approx 0.3.$$

Values $\ell \geq 1$ require order-1 or larger; only $\ell = 0$ fits inside the nuclear range at this energy [6].

Bibliography

[1] R. A. Dunlap, *An Introduction to the Physics of Nuclei and Particles* (2nd ed.), IOP Publishing, Bristol (2023), DOI: 10.1088/978-0-7503-6094-4, Ch. 3 (Nuclear composition and size).

[2] W. Demtröder, *Nuclear and Particle Physics*, Undergraduate Lecture Notes in Physics, Springer, Cham (2023).

[3] S. Petrera, *Problems and Solutions in Nuclear and Particle Physics*, UNITEXT for Physics, Springer, Cham (2019).

[4] F. Terranova, *A Modern Primer in Particle and Nuclear Physics*, Oxford University Press (2021).

[5] S. D'Auria, *Introduction to Nuclear and Particle Physics*, Undergraduate Lecture Notes in Physics, Springer, Cham (2018).

[6] K. S. Krane, *Introductory Nuclear Physics*, Wiley, New York (1988).

[7] R. Hofstadter, "Electron scattering and nuclear structure," Rev. Mod. Phys. **28**, 214 (1956).

[8] H. F. Ehrenberg, R. Hofstadter, U. Meyer-Berkhout, D. G. Ravenhall, and S. E. Sobottka, "High-Energy Electron Scattering and the Charge Distribution of Carbon-12 and Oxygen-16," Phys. Rev. **113**, 666 (1959).

[9] H. Yukawa, "On the interaction of elementary particles. I," Proc. Phys.-Math. Soc. Japan **17**, 48 (1935).

[10] R. D. Woods and D. S. Saxon, "Diffuse surface optical model for nucleon-nuclei scattering," Phys. Rev. **95**, 577 (1954).

[11] H. G. J. Moseley, "The high-frequency spectra of the elements," Phil. Mag. **26**, 1024 (1913); **27**, 703 (1914).

[12] C. F. von Weizsäcker, "Zur Theorie der Kernmassen," Z. Phys. **96**, 431 (1935).

[13] P. Cappellaro, *Introduction to Applied Nuclear Physics* (MIT OpenCourseWare / LibreTexts), CC BY-NC-SA 4.0.

[14] J.-L. Basdevant, J. Rich, and M. Spiro, *Fundamentals in Nuclear Physics: From Nuclear Structure to Cosmology*, Springer, New York (2005).

[15] D. Tong, *Particle Physics*, Lecture notes (University of Cambridge / CERN school notes).